PORE-SCALE MODELING OF ENHANCED VAPOR DIFFUSION IN POROUS MEDIA

Stephen W. Webb
Environmental Restoration Technologies Department 6621
Sandia National Laboratories
Albuquerque, New Mexico 87185-0719, USA

Clifford K. Ho
Geohydrology Department 6115
Sandia National Laboratories
Albuquerque, New Mexico 87185-1324, USA

ABSTRACT

Vapor diffusion in porous media in the presence of its liquid has often been analyzed like air diffusion. The diffusion rate is much lower than in free space due to the presence of the porous medium and any liquid present. However, enhanced vapor diffusion has also been postulated such that the diffusion rate may approach free-space values. The mechanisms postulated to lead to this enhancement include condensation/evaporation across isolated liquid islands in the porous media and an increased temperature gradient in the gas phase. In order to try to understand the mechanisms involved in such an enhancement, pore-scale models have been developed. Vapor diffusion in the presence of liquid islands has been evaluated for a one-dimensional linear system, a two-dimensional pore, and a small two-dimensional pore network under a concentration gradient. The simulations show that significant enhancement of vapor diffusion is indeed possible in the presence of liquid islands, while air diffusion decreases slightly. While the present pore-scale model indicates that enhanced vapor diffusion is possible, only experimental data can confirm the relevant processes.

I. INTRODUCTION

Vapor diffusion in porous media may be significant in the flow of subsurface fluids and in the transport of contaminants. In many environmental remediation and waste isolation applications, such as removal of nonaqueous phase liquid (NAPL) contaminants from low-permeability layers in the subsurface, vapor diffusion is the limiting transport mechanism (Ho and Udell, 1992, Webb and Phelan, 1997). Diffusion of vapors may also be important in high-level nuclear waste repositories, in the drying of paper and textiles, and in agricultural processes.

Gas diffusion in porous media is generally significantly smaller than in free space due to the presence of the porous medium. The flow area for gas-phase diffusion is reduced by the presence of the solid particles, by the presence of any liquid, and by the fact that the flow path for diffusion in a porous medium is more tortuous than in free space. Using Fick's law, gas diffusion in a porous media may be expressed as follows

$$F_i = -\tau\phi S_g D_{12}\rho_g \nabla\omega_i = -\beta D_{12}\rho_g \nabla\omega_i \qquad (1)$$

where D_{12} is the free-space diffusion coefficient at the pressure and temperature of interest. The product of the tortuosity coefficient, τ, the porosity, ϕ, and the gas saturation, S_g, is often referred to as the porous media factor, β. Since the tortuosity coefficient and the porosity are always less than 1, and the gas saturation is a maximum of 1, the porous media factor, β, is always much less than 1, and gas diffusion in a porous medium is usually significantly lower than in free space.

In contrast, it has been postulated that diffusion of a condensable vapor in the presence of its liquid may be considerably enhanced compared to gas diffusion rates and may approach or even exceed free-space values. (In the present discussion, *gas* refers to a non-condensible inert gas under the conditions of interest, or air. *Vapor* refers to the gas phase which may have a liquid phase present, or water vapor). Enhanced vapor diffusion was first considered by Philip and deVries (1957) for soils. Jury and Letey (1979) estimated that the value of β is of the order 1.0 resulting in considerable enhancement of vapor diffusion compared to gas diffusion. When β equals 1.0, diffusion is not affected by the porous medium at all and is equal to the value for free-space diffusion. Enhanced vapor diffusion is commonly assumed in soil science but has seen limited use in engineering applications.

The mechanisms for such an enhancement are postulated to include local condensation and evaporation at isolated liquid "islands" within the porous medium. Instead of forming a barrier to vapor diffusion, these liquid islands enhance the vapor diffusion rate, or apparent diffusion rate, by reducing the effective diffusion path length. Due to local vapor pressure lowering, condensation occurs at the upstream end of the island, while evaporation occurs on the downstream end, even for isothermal conditions. The difference in curvature of the meniscus at each end of the liquid island, and the capillary pressure, will result in a liquid pressure difference across the liquid island causing liquid flow.

Another mechanism postulated to contribute to this enhancement is an increased temperature gradient in the gas phase compared to the average temperature gradient in the equivalent porous medium due to the

DISCLAIMER

lower conductivity of the gas phase. This increased temperature gradient mechanism will not be discussed in the present study since no temperature gradient is imposed. This contribution will be addressed in subsequent work.

Ho and Webb (1997) have reviewed enhanced vapor diffusion mechanisms, models and data. They concluded through the use of a simple pore-scale model that enhancement is indeed possible, although direct measurements are not available. Based on this review, additional modeling and experiments at multiple length scales were proposed to try to understand the mechanisms involved. The experiments are currently underway. Pore-scale modeling is discussed in the present paper.

Interestingly, the same phenomena of enhanced vapor diffusion due to liquid island processes has been noted in the capillary condensation literature. Due to vapor pressure lowering effects, condensation occurs in small pores in a porous media. Weisz (1975) has estimated the apparent increase in vapor diffusivity due to liquid island effects. As noted by Weisz (1975), this effect was first experimentally discovered by Carman and coworkers between 1950 and 1952 (which is before Philip and deVries). Representative models include Lee and Hwang (1986), who developed a liquid island model for flow in a capillary, and Rajniak and Yang (1996), who proposed a pore network model for capillary condensation. However, to the authors' knowledge, a detailed investigation of the pore processes presented in this study has not been performed.

In the present investigation, pore-scale modeling of vapor diffusion in porous media is considered including the interactions of the vapor with the liquid islands. The parameters selected for this investigation are more typical of soils than for capillary condensation applications, which typically involve much smaller pores. The Dusty-Gas Model is used to simulate air-vapor advection and diffusion in a pore network including Knudsen and ordinary (Fickian) diffusion (Webb, 1997). Surface diffusion effects are not considered. Kelvin's equation is used to estimate vapor pressure lowering effects at the liquid island/gas-liquid interface, and the Young-Laplace equation is used to evaluate gas-liquid pressure differences at either end of the liquid island. Concentration gradients are applied to the pore-scale model to calculate the vapor and air flow rates which are then compared to pure gas diffusion in the porous medium and in free space. No temperature or pressure gradients are imposed in the present study although the model allows for these gradients.

In somewhat similar work, Steele and Nieber (1994a,b) performed some gas diffusion pore-scale modeling in an unsaturated medium. However, their investigation only considered gas diffusion (as opposed to vapor diffusion) and the transport of dissolved gas through stationary liquid; vapor diffusion effects were ignored. As will be evident from the results shown in this paper, vapor diffusion, along with the condensation/evaporation across liquid islands, may also influence gas diffusion. The present emphasis is on vapor diffusion, although some gas diffusion results are also presented.

In another recent study, Plumb and Prat (1992) evaluated the effective vapor diffusion coefficient for drying conditions using a pore-scale model. Their model calculated significant enhancement compared to gas diffusion rates, similar to enhanced vapor diffusion. However, the increase in vapor diffusion is due to evaporation from the liquid islands present in the pore-scale model. Capillary pressure and vapor pressure lowering processes were not considered, and condensation on the upstream end of the liquid island was not evaluated. This model is discussed in more detail in Prat (1993). Enhanced vapor diffusion as defined in this paper is a steady-state process in which the mass of the liquid island is constant. The enhanced vapor diffusion considered by Plumb and Prat (1992) is a transient process driven by evaporation from the liquid as discussed in more detail later.

II. PORE-SCALE ANALYSIS

A. Simple Approach

Before embarking on a discussion of the current pore-scale model, it is instructive to briefly review the pore-scale analysis presented by Ho and Webb (1997); this simple model is depicted in Figure 1. Ho and Webb used this simple pore-scale model to estimate the steady-state mass flow of water vapor in various pore-scale transport paths. The first path considered (A-A) is flow through the liquid island due to water vapor condensation and evaporation, which has been postulated as a mechanism for enhanced vapor diffusion (Philip and deVries, 1957; Jury and Letey, 1979). The second path (B-B) in Figure 1 is due to Fickian diffusion around the liquid island. The mass flux through the liquid island was based on an energy balance between the heat added to the upstream interface by the latent heat of condensation and heat conduction in the liquid island away from the upstream interface.

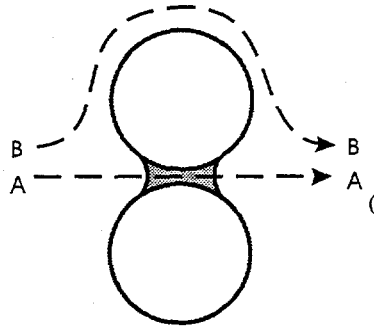

Figure 1
Pore-scale Transport Paths
(A-A) Enhanced Vapor Diffusion
(B-B) Fickian Diffusion

The results from that simple pore-scale model indicated that net water vapor mass transfer through the liquid islands may be about an order of magnitude higher than water vapor transport around the liquid island by Fickian diffusion, or

$$\frac{m_{v,liquid\ island}}{m_{v,Fickian\ diffusion}} \sim 10 \ . \qquad (2)$$

While the existence of these mechanisms remains to be experimentally demonstrated, the possibility exists based on this simple analysis, and more detailed pore-scale modeling of enhanced vapor diffusion mechanisms is presented below.

B. Model Description

The above result is very instructive, indicating that flow through liquid islands may indeed contribute significantly to "apparent" vapor-phase diffusion. In the present investigation, a more rigorous pore-scale numerical model is developed to investigate the fundamental processes involved in the enhancement of vapor diffusion in porous media. Conservation of mass, flux, and energy are considered in the gas, liquid and solid phases. At the gas-liquid interface, capillary pressure due to local curvature is considered, and vapor pressure lowering is included as described below.

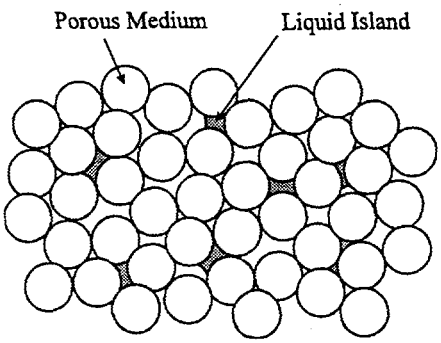

Figure 2
Porous Medium Conceptual Model

Conceptual Model. The conceptual model employed in the present study is depicted in Figure 2. The porous media is considered to be a series of randomly-arranged spheres. Heat transfer occurs between the spheres due to particle-to-particle contact, while flow of gas occurs around the spheres and around any liquid islands present. The liquid saturation is assumed to be low such that the liquid is confined to pendular rings, or "liquid islands", and no global flow of liquid occurs. Gas and vapor flow due to advection and diffusion can occur due to pressure, temperature, and/or concentration gradients.

Simplified Representation. Figure 3 shows the simplified representation that was used in the present study based on the conceptual model shown in Figure 2. The particles are assumed to be arranged in rows, and the liquid islands are assumed to occur on a regular basis. Symmetry is invoked as indicated by the dashed-line box in the figure. A two-dimensional representation has been used for simplicity, and the solid particles are represented as cylinders.

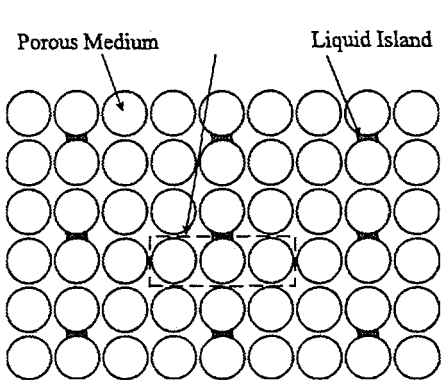

Figure 3
Porous Medium Simplified Representation

Numerical Method. For the present study, the TOUGH2 (Pruess, 1991a) code has been employed. TOUGH2 is a widely-used code for simulating flow and transport in fractured and porous media. Typical applications include environmental remediation, nuclear waste isolation, and geothermal processes (Pruess, 1995). TOUGH2 is an integrated finite difference code that solves mass, flux, and energy conservation equations for fluid flow in a porous media. The formulation for an arbitrarily-shaped domain, V, is as follows for the accumulation, flux, and source terms (Pruess and Narasimhan, 1985):

$$\frac{d}{dt}\int_V M_\kappa dv = \int_\Gamma F_\kappa \cdot n \, d\Gamma + \int_V q_\kappa \, dv \tag{3}$$

where κ is water, air, or heat. The fluid mass accumulation term is

$$M_\kappa = \phi \sum_{\beta=1}^{2} S_\beta \rho_\beta \omega_{\beta,\kappa} \tag{4}$$

where β is the liquid and gas phases. The heat accumulation term is

$$M_3 = (1-\phi)\rho_R C_R T + \phi \sum_{\beta=1}^{2} S_\beta \rho_\beta u_\beta \, . \tag{5}$$

The flux term for the gas phase is based on the Dusty Gas Model (DGM) (Mason and Malinauskas, 1983), which considers advection, Fickian diffusion, and Knudsen diffusion, including the coupling between the various mechanisms. The original version of TOUGH2 uses an advective-dispersive formulation in which the fluxes from the various mechanisms is simply added together; the coupling among the mechanisms is not considered. The difference between these two formulations is discussed in detail by Webb (1997) including quantification of the differences in the various mechanisms. For the DGM, the gas mass flux of component κ in the gas phase for a binary system can be written as

$$F_\kappa = J_\kappa M_\kappa = -M_\kappa \frac{D_\kappa^K D_{\kappa\kappa^*} \frac{P_g}{RT} \nabla x_\kappa}{D^*} - M_\kappa \frac{D_\kappa^K (D_{\kappa\kappa^*} + D_{\kappa^*}^K) x_\kappa \frac{(\nabla P_g - \rho_g g)}{RT}}{D^*} - M_\kappa x_\kappa \frac{kP_g}{\mu_g} \frac{(\nabla P_g - \rho_g g)}{RT} \tag{6}$$

where κ=air or water vapor, $\kappa^* \neq \kappa$, and

$$D^* = D_{\kappa\kappa^*} + x_\kappa D_{\kappa^*}^K + x_{\kappa^*} D_\kappa^K \, . \tag{7}$$

The above equations for the Dusty Gas Model are written in terms of mole fractions rather than mass fractions because mole fraction is a more natural variable for diffusion.

In equation 6, the flux of component κ consists of a diffusive flux (first and second terms) and an advective flux (third term). The diffusive flux has ordinary diffusion (mole fraction gradient) and Knudsen diffusion (pressure gradient) components.

The flux term for the liquid phase is simply

$$F_l = - \frac{k}{\mu_l} \rho_l \omega_{l,\kappa} (\nabla P_l - \rho_l g) \quad (8)$$

where the assumption of separation of phases, which is discussed below, has been used (relative permeability = 1.).

The heat flux term is simply

$$F_3 = - k \nabla T + \sum_{\substack{\beta = l,g \\ \kappa = 1,2}} h_{\beta,\kappa} F_{\beta,\kappa} \quad (9)$$

Capillary pressure and vapor pressure lowering effects can be included in TOUGH2. By setting the control volume porosity equal to 0.0 or 1.0, the control volumes can be used to represent solid or fluid regions.

TOUGH2 models elements, or control volumes, and connections between the centers of these elements. The standard version assumes that if more than one phase is present in an element, the phases are completely mixed. In the present model, the only elements which contain more than one phase are the elements at the ends of the liquid island, or the interface volumes. For simplicity, the liquid island length is defined so the interface is exactly in the middle of an interface element, so the element is half liquid and half gas. Due to capillary forces and the pore-scale nature of the present model, the phases will be separate. The flow path from the interface volume to the gas phase will be entirely gas. Similarly, the flow path between the interface element and the liquid island will be all liquid. The flow path transport parameters used in the code, such as the saturation and fluid transport properties, were modified to reflect separate, rather than mixed, phases.

The applicability of the Dusty Gas Model to the pore scale needs to be discussed. In particular, the simple Knudsen diffusion representation of elastic molecule-wall collision breaks down as the pore dimension decreases, and Knudsen diffusion no longer applies. This diffusion regime for small dimensions is called configurational diffusion and is often encountered in diffusion through membranes. Cunningham and Williams (1980) discuss the transition between the two regimes and conclude that the approximate transition is at a capillary radius of about 50 Å, or 0.005 μm. As will be seen later, the pore sizes considered in the present study are considerably larger than this transition radius, so the Dusty Gas Model is applicable. Note that Sotirchos and Burganos (1988) have also used the Dusty Gas Model in their multicomponent diffusion analysis in pore networks.

Other numerical approaches, including lattice-gas methods, could be applied to the present pore-scale problem. These methods may be more accurate than the present approach but at a cost of more model development time and effort. As discussed by Ho and Webb (1997), the existence of and the processes involved in enhanced vapor diffusion are still being evaluated. In fact, enhanced vapor diffusion has never been directly calculated by a mechanistic model, such as the one developed here. When and if the mechanisms involved become clear, and if significant enhancement is experimentally confirmed, development of a more accurate code may be appropriate. Until that time, however, an approximate method, such as outlined in this paper, is an efficient approach for initial investigations.

Table 1
Pore-Scale Model Parameters

Dimensions	
Pore Radius	5 μm
Equivalent Permeability	2×10^{-12} m^2
Particle Radius	50 μm
Model Porosity	0.322
Diffusion	
Binary Diffusion Coefficient	2.42×10^{-5} m^2/s
Knudsen Diffusion Coefficient - Air	1.54×10^{-3} m^2/s
Knudsen Diffusion Coefficient - Vapor	1.96×10^{-3} m^2/s

Model Geometry. Three different geometries were studied:

1) one-dimensional linear system;
2) two-dimension single pore; and
3) two-dimensional pore network.

The use of the one-dimensional linear system allows for a simple evaluation of the effect of the liquid island on the vapor diffusion rate, while the two-dimensional single pore includes the variation in cross-sectional area in a pore. Finally, the two-dimensional pore network considers the competition between vapor diffusion through open pores and through liquid islands. The model parameters, including the nodalization, are discussed in the next section.

C. MODEL PARAMETERS

The model parameters are summarized in Table 1 and are discussed in detail below.

Pore-Scale Dimensions. The dimensions for the current pore-scale model are chosen to be consistent with the enhanced vapor diffusion data tabulated by Jury and Letey (1979). An average value of the capillary head (pressure) data is approximately 300 cm (range of < 10 cm to 5 x 10^4 cm with a median of 269 cm). Using Young-Laplace's equation for the pressure difference across a curved surface (Dullien, 1992)

$$\Delta P = \frac{2\sigma}{r} \quad (10)$$

and an air-water surface tension, σ, at 20°C of 72.8 dynes/cm, a typical minimum pore radius is 5×10^{-6} m, or 5 μm.

In the two-dimensional present simulations, additional assumptions have been made in the numerical model in the application of TOUGH2. The spheres are represented by an octagonal geometry; an octagon was selected rather than a square in order to approximate some of the variation of the pore cross-sectional area. A non-symmetrical octagon was employed such that the faces parallel to the x and y directions have a slightly different length than the diagonal faces. This shape allows for the use of a regular grid consisting of square elements except at the diagonal faces of the solid; square elements are desirable when using the 9-point scheme discussed below. On the diagonal faces, the square elements are divided into equal triangles, one which is solid and one which is fluid.

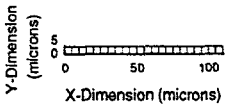

(a) One-Dimensional Linear Model

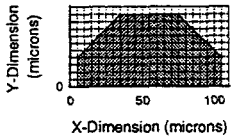

(b) Two-Dimensional Single Pore

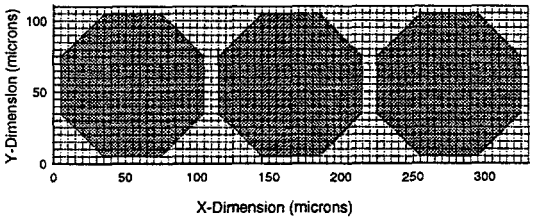

(c) Two-Dimensional Pore Network

Figure 4
Pore-Scale Models

The particle diameter in the numerical model has been chosen to be 50 μm, which supports the use of square elements, and gives a reasonable model porosity value of 0.322. An octagonal representation of a cylinder is used in the TOUGH2 model. The height and width of the octagon is 100 μm, consistent with the particle diameter.

The standard version of TOUGH2 employs a 5-point stencil to connect the elements in the x- and y-directions. This numerical scheme is not appropriate for flow along the diagonal surfaces in the model or for flow between the square and triangular elements. Therefore, a 9-point differencing scheme has been used which adds diagonal connections between elements. The main advantage of the 9-point scheme in the present model is connections parallel to the diagonal surfaces of the solid particles which allows for a more reasonable octagonal shape rather than a "stair-step" surface. As shown by Pruess and Bodvarsson (1983) and Pruess (1991b), grid orientation effects can also be significant for the 5-point scheme, especially when a diagonal surface is present; these effects are greatly reduced when a 9-point scheme is employed.

The nodalization of the three models is shown in Figure 4. For simplicity, the boundary elements are not shown. For the one-dimensional linear system, 24 square elements were used including boundary elements on either end of the model; the effective model length is 110 μm (22 active elements x 5 μm). Making use of symmetry, the two-dimensional single-pore model is 24 elements long and 11 elements wide, and the effective model dimensions are 110 μm long by 55 μm wide. Finally, the two-dimensional pore network is 68 elements long and 22 elements wide. The two end columns represent boundary conditions, so the effective dimensions are 330 μm long and 110 μm wide.

Permeability. The analogy between Darcy's law and laminar flow between parallel plates has been used (de Marsily, 1986), or

$$k = \frac{r^2}{12} \tag{11}$$

and the equivalent permeability for the minimum pore dimension of 5 μm is 2×10^{-12} m^2.

The analogy between Darcy's law and laminar flow between parallel plates is based on the distance between solid surfaces and results in a parabolic velocity profile based on a constant flow area. In the present model, the flow area varies dramatically in the direction of flow, so the suitability of a parabolic velocity profile is questionable. This problem has been at least partially addressed by Brown et al. (1995), who calculated velocity profiles between undulating surfaces of a hypothetical fracture. For the present particle geometry, the results from Brown et al. (1995) indicate that, under steady flow conditions, the fluid velocity profile will be nearly parabolic at the pore throat and "Gaussian" at the wider part of the channel. The fluid velocity is also dependent on the shape of the channel which is not captured in the analogy. Nevertheless, for simplicity, locally parabolic velocity profiles will be implicitly assumed in the present model by relying on the parallel plate analogy. Because the flow modeling is primarily concerned with diffusion, the error introduced through the use of this analogy should be small.

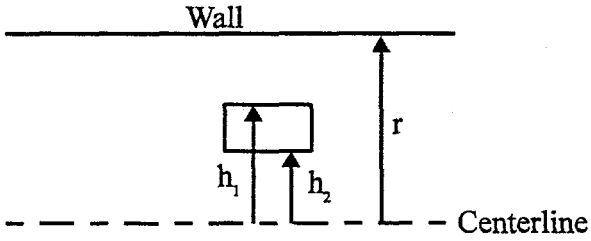

Figure 5
Effective Permeabilities for a Parabolic Velocity Profile

Accepting the parallel plate analogy for the present study, the effective permeability must vary normal to the flow direction in order to produce the desired parabolic velocity profile. The effective permeability for a given element can be derived by integrating the velocity profile over the respective coordinates as shown in Figure 5. For an element with coordinates h_1 and h_2 from the center of the channel to the edges of the element, the effective permeability is given by

$$k = \frac{1}{2}\left(\frac{r^2}{4} - \frac{1}{12}\left(h_2^2 + h_1 h_2 + h_1^2\right)\right) . \tag{12}$$

For any given element, there may be different radii in the horizontal and vertical directions as indicated in Figure 6. Assuming parabolic profiles in both the horizontal and vertical directions, these radii result in different horizontal (h) and vertical (v) effective permeabilities according to the above relationship.

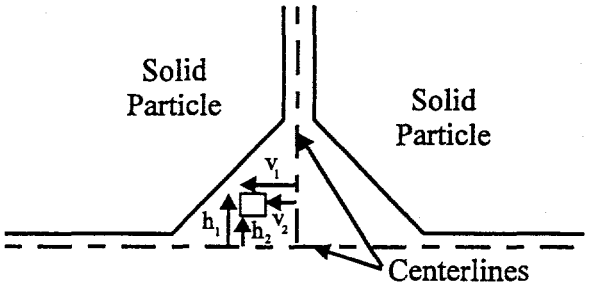

Figure 6
Definition of Horizontal and Vertical Effective Permeabilities

Diffusion. The binary diffusion coefficient for the present study is 2.42 x 10^{-5} m^2/s at the analysis conditions of 10^5 Pa and 20°C (Pruess, 1991a). The Knudsen diffusion coefficient is calculated by the following formula from Cunningham and Williams (1980) for perfectly diffuse molecule-wall collisions (coefficient of diffuse reflection = 1.0), or

$$D_\kappa^K = \frac{2}{3} r v \tag{13}$$

where v is the mean molecular speed

$$v = \left(\frac{8 k_B T}{\pi M_\kappa} \right)^{1/2} \tag{14}$$

and k_B is Boltzmann's constant. For the present minimum pore dimension of 5 μm, this equation gives the value of 15.4 cm^2/s or 1.54 x 10^{-3} m^2/s for air at 20°C. For water vapor, the value for air can simply be scaled by the inverse of the square root of the ratio of molecular weights, resulting in a value of 1.96 x 10^{-3} m^2/s. No modifications of the diffusion coefficients are made to account for the presence of the porous medium since the present model is a pore-scale approach.

Similar to the effective permeability discussion, any given element may have different radii in the horizontal and vertical directions. However, as discussed in detail by Cunningham and Williams (1980), the fluid velocity from Knudsen diffusion is uniform and is independent of distance from the wall. Therefore, the Knudsen diffusion coefficient is simply a function of the horizontal and vertical radii and, unlike the effective permeability, is *not* a function of the local coordinates.

Liquid Island. The model for the liquid island is one of the major pieces of the current pore-scale analysis. Capillary pressure across the gas-liquid interface and vapor pressure lowering is included. Capillary pressure is a function of position, or length, of the liquid island as illustrated in Figure 7; the capillary pressure near the minimum pore dimension (A), which corresponds to a short liquid island, is much higher than for a much larger dimension (B), or a much longer liquid island. By geometry, the radius of curvature for a given contact angle can be calculated as a function of position, or equivalently, liquid island length. Assuming a contact angle of 0°, the capillary pressure as a function of position is shown in Figure 8, where the coordinate (x) is zero at the minimum pore dimension. A maximum x/R value of 0.75, where R is the particle radius, was used in the development of the capillary pressure function.

Figure 7
Schematic for the Liquid Island
Capillary Pressure Function

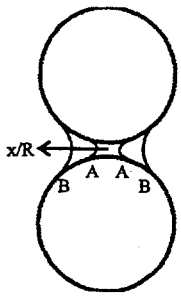

The capillary pressure due to the gas-liquid interface results in local vapor pressure lowering due to the curvature (Dullien, 1992). This effect can be quantified through Kelvin's equation which can be written as

$$P_v = f_{VPL} P_{sat} \tag{15}$$

where

$$f_{VPL} = \exp\left(\frac{M_w P_c}{\rho_w R T} \right) \tag{16}$$

where the capillary pressure is defined as P_{liquid} minus P_{gas} which is negative. For the assumed uniform temperature of 20°C, the saturated water vapor pressure is 2337 Pa. For the maximum capillary pressure of about 30 kPa as shown in Figure 8, the vapor pressure lowering factor is 0.99978, or a minimum vapor pressure of 2336.5 Pa, which results in a maximum vapor pressure lowering of only about 0.5 Pa.

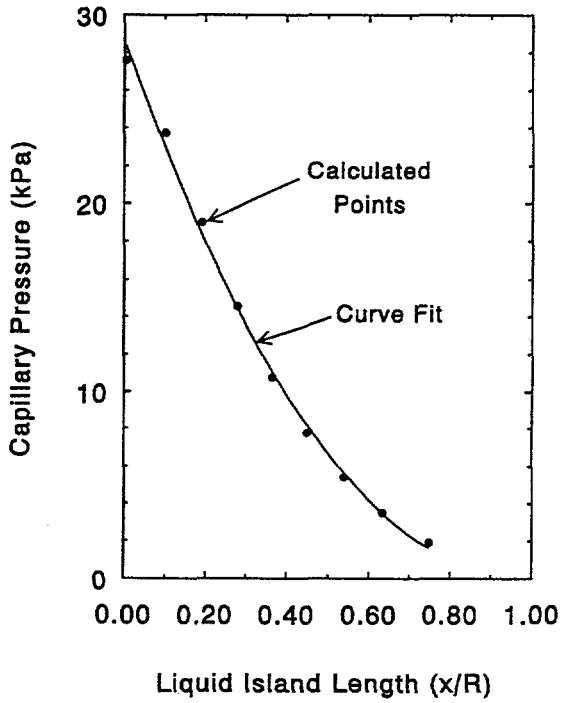

Figure 8
Liquid Island Capillary Pressure Function

Even though the magnitude of vapor pressure lowering is small in magnitude, and its effect is often ignored, it can have a large influence on enhanced vapor diffusion. For example, flow through liquid islands is driven by condensation and evaporation on both ends of the liquid island. Without vapor pressure lowering, enhanced vapor diffusion as defined in this study does not occur.

Boundary Conditions. The boundary conditions consist of left-hand and right-hand side boundary columns with uniform conditions. A small concentration gradient is imposed across the model for the present simulations; zero pressure and temperature gradients are assumed. Specification of the boundary conditions, including the magnitudes, and the influence of "assisting" or "opposing" boundary conditions is of considerable interest. These factors will be studied further as development of the pore-scale model continues.

The objective of the present investigation is to calculate steady-state vapor diffusion through the various models such that there is no net change in the liquid island mass. Transient vapor diffusion, including net condensation or evaporation of liquid, is often encountered in applications such as drying. Plumb and Prat (1992) evaluated the effective vapor diffusion coefficient, or enhanced vapor diffusion, under transient drying conditions. However, in their situation, the definition of enhanced vapor diffusion is complicated because the flow of vapor into and out of the model changes with time and position. An investigation of this topic is currently underway.

In order to calculate steady-state vapor diffusion, condensation and evaporation rates on the liquid island must be equal. For a zero concentration gradient, no condensation or evaporation should occur on the liquid island at equilibrium. This equilibrium condition is slightly dependent on the liquid island capillary pressure, and therefore the liquid island length, due to vapor pressure lowering effects, and the vapor pressure is slightly lower than saturation. A small concentration gradient is imposed to calculate vapor diffusion which is centered around this equilibrium condition. This equilibrium condition results in slightly superheated conditions ($P_{vap} < P_{sat}$) at the model boundaries. The concentration gradient is sufficiently small such that the vapor pressure at the boundaries is always less than P_{sat} to avoid condensation and evaporation at locations other than the liquid island. Within this limit, the results scale with the magnitude of the concentration gradient such that any enhancement is gradient independent. In all cases, a false transient was performed to achieve steady-state conditions such that mass flow rates into and out of the model were essentially the same.

III. RESULTS

The simulation results for all three models are presented in this section. Some of the results from the pore-scale model are compared to the free-space gas diffusion results calculated by Fick's law, or

$$F_{i,Fickian\ diffusion} = -D_{12}\,\rho_g\,\nabla\omega_i \qquad (17)$$

with an air-water vapor density of 1.178 kg/m^3 and the binary diffusion coefficient in Table 1. For a binary air-water vapor system, the diffusive mass fluxes according to Fick's law will be equal and opposite. The assumption of equal and opposite mass fluxes in a binary system is inconsistent with Graham's law of diffusion as discussed later.

One-dimensional Linear System. A one-dimensional linear model based on the minimum pore dimension has been used as the initial model investigating enhanced vapor diffusion as depicted in Figure 4. A liquid island is centered in the one-dimensional model, and the appropriate boundary conditions are imposed as discussed above. Because the flow area is uniform, the capillary pressure is constant, and there is no unique liquid island position. In this case, there is also a stability concern, since any change in the liquid island length has no effect on the liquid island capillary pressure or vapor pressure lowering. In order to keep the liquid island in the center of the linear model, and to allow feedback between the liquid island length and condensation/evaporation processes, the two-dimensional capillary pressure curve shown earlier in Figure 8 was used.

When there is no liquid island, pure gas diffusion occurs. The present simulations use the Dusty Gas Model which is more appropriate to a porous medium than Fick's law as discussed by Webb (1997). For Fick's law, the water vapor and air diffusive mass fluxes are equal and opposite. However, in porous media, Graham's law of diffusion applies, and the diffusive mass fluxes will be proportional to the square root of the ratio of the molecular weights (Mason and Malinauskas, 1983). (Also note that the mole fluxes are not equal). In the present simulations, the vapor diffusive mass flux is 2% *lower* than Fick's law, while the air diffusive mass flux is 25% *higher* than Fick's law; this difference is consistent with the ratios predicted by Webb (1997). As a result of the unequal diffusive mass fluxes, the porous media factors will be different for water vapor and for air.

The enhancement in vapor diffusion as a function of liquid island length is given in Figure 9. Enhancement is defined as the vapor diffusion rate compared to the all-gas case. As shown in the figure, vapor diffusion may be significantly enhanced in the presence of a liquid island. The longer the liquid island, the greater the enhancement.

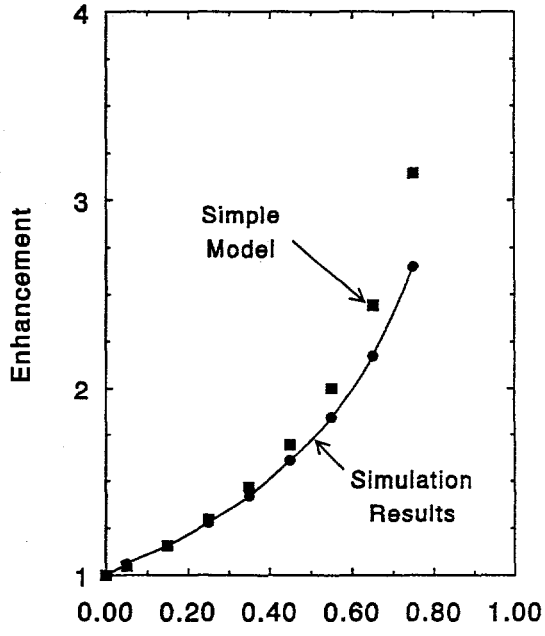

Figure 9
Enhancement of Vapor Diffusion
for the One-Dimensional Linear Model

Also shown in Figure 9 is a function which is simply proportional to the length of the vapor diffusion path in the model, assuming that the liquid island has zero resistance (note that the total model length is 110 μm whereas the particle diameter is 100 μm). The shortened diffusion path length model overestimates the enhancement given by the simulations because the liquid island resistance is neglected.

Two-dimensional Single Pore. Figure 4 shows the two-dimensional single pore model which includes variation in cross-sectional area in a pore. Initial results with no liquid island (all gas) indicate that the porous media factor, β, for water vapor is 0.147 compared to Fick's law value in free space. As mentioned above, the porous media factor for air will be different than for water vapor and is 0.186 for the all-gas case. These porous media factors (air and water vapor) are reasonably consistent with the theoretical value predicted by Ryan et al. (1981) of approximately 0.17 and with the experimental data shown by them.

Figure 10 plots the enhancement in vapor diffusion for the two-dimensional single pore model. Similar to the one-dimensional linear results, vapor diffusion is significantly enhanced when a liquid island is present and increases with liquid island length. The "kink" in the results at a liquid island fractional length of 0.40 is due to the change in the model pore flow area at that location caused by the octagonal representation of the solid particles. In the present case, the enhancement is up to an order of magnitude for the longest liquid island considered. Simplified model results are also shown in Figure 10. This model simply integrates the diffusion equation over the gas portion of the model including the variation in pore area, assuming that the liquid island portion has zero resistance. This simplified model agrees very well with the simulations.

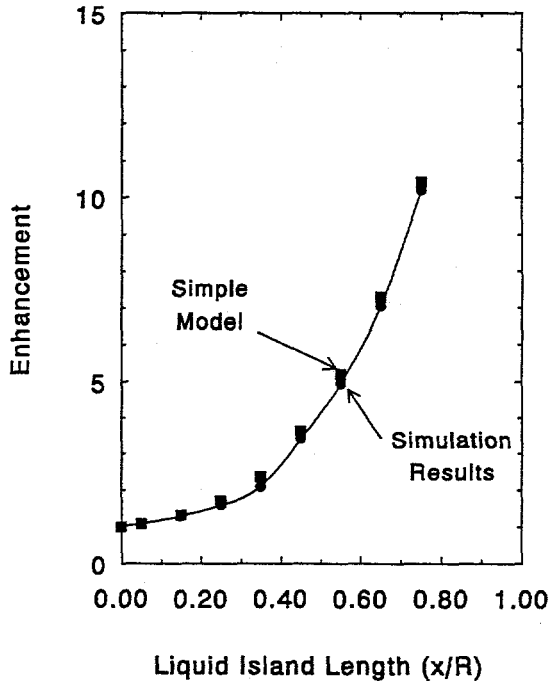

Figure 10
Enhancement of Vapor Diffusion
for the Two-Dimensional Single Pore Model

Figure 11 shows the porous media factor, β, for vapor diffusion. The value increases from the all-gas value of 0.147 to a maximum value of 1.5, or 50% ***larger*** than the free-space value. Recall that Jury and Letey (1979) estimated that the porous media factor would be approximately 1.0. Because this model only considers a single pore, there is no diffusion of air from one boundary to the other (dissolved gas diffusion is not included). Air diffusion results will be presented for the two-dimensional pore network which is discussed next.

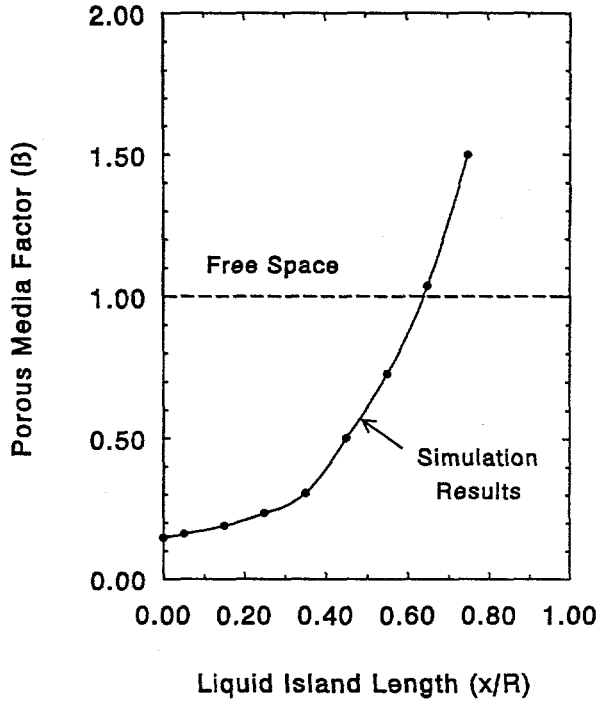

Figure 11
Vapor Diffusion Porous Media Factor (β)
for the Two-Dimensional Single Pore Model

Two-dimensional Pore Network. The two-dimensional pore network is the most general of the three models described in this study and is intended to investigate the competition between open pores and liquid islands. In this model, only a single liquid island is introduced, so any overall enhancement will be small. In addition to the competition for vapor diffusion between the liquid island and open pores, this model addresses diffusion of the gas phase (air) in the presence of a liquid island.

The case for gas-only diffusion, or diffusion without liquid islands, gives results identical to the two-dimensional single pore for the porous media factor. Because the boundary conditions specified no total pressure gradient, all flow is due to diffusion. The mass flow vectors for water vapor and air are given in Figure 12. Because of the concentration gradient imposed, vapor diffuses from right-to-left, while air diffuses from left-to-right. The mass flux of air is higher than the mass flux of water vapor consistent with Graham's law of diffusion as discussed earlier.

For cases with a liquid island, even though the boundaries have the same total pressure, advection and Knudsen diffusion occur. While vapor essentially flows "through" the liquid island, gas (air) is effectively

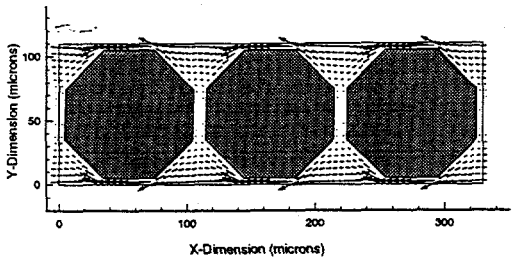

(a) Water Vapor Total Mass Flow Vectors

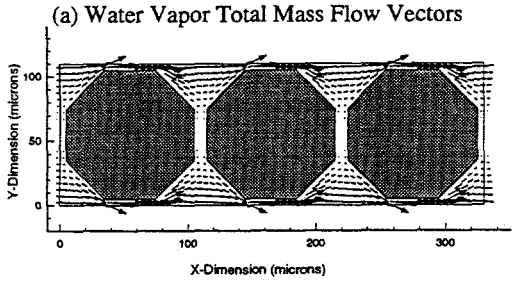

(b) Air Total Mass Flow Vectors

Figure 12
Mass Flow Vectors
for the Two-Dimensional Pore Network Model
For All Gas Conditions

blocked by the liquid island and builds up on the upstream end of the island. Because air is stagnant at the liquid island, diffusion away from the liquid island caused by the build up of air must be balanced by advection towards the liquid island. Therefore, there are diffusion, advection, and Knudsen diffusion contributions to vapor and air flow.

Figures 13a and 13b show the mass flow vectors for water vapor and air in the case of the longest liquid island, respectively. The liquid island is assumed to be in the top pore throat of the center particle. Three velocity vector plots are shown for the total, diffusive, and advective mass velocity contributions using the same scale. Knudsen mass velocity fluxes are not shown since their contribution is small in the present simulations. Vapor essentially diffuses "through" the liquid island via condensation/evaporation mechanisms as indicated by the vector plots. The total vapor mass flow is dominated by diffusive fluxes; the advective contribution is small as indicated by the vector plots. Upstream, the liquid island "pulls" vapor from the open-pore side of the model, even though the vapor flow path is considerably larger than if the vapor flowed straight through. On the downstream portion, the vapor flux from the liquid island is "pushed" back to the open-pore side. The vapor mass velocity vectors are slightly larger than for the all-gas case indicating enhanced vapor diffusion. For the air, the flow pattern is just about the opposite of the vapor. Since the liquid island effectively blocks air flow, the air must go around the liquid island, and air is stagnant next to the interface. At the right end of the liquid island, vapor diffuses toward the

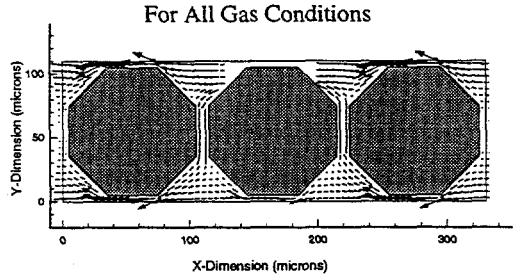

(a) Water Vapor Total Mass Flow Vectors

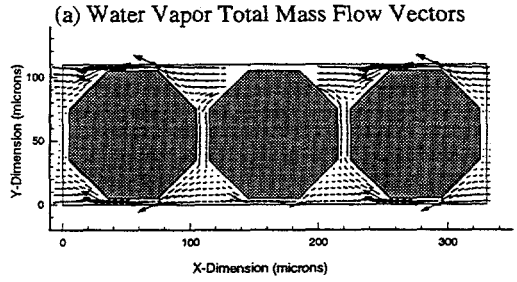

(b) Water Vapor Diffusion Mass Flow Vectors

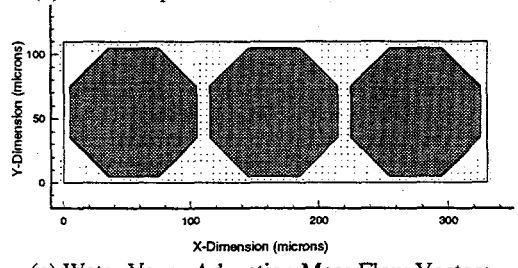

(c) Water Vapor Advection Mass Flow Vectors

Figure 13a
Water Vapor Mass Flow Vectors
for the Two-Dimensional Pore Network Model
For a Liquid Island Length of x/R=0.75

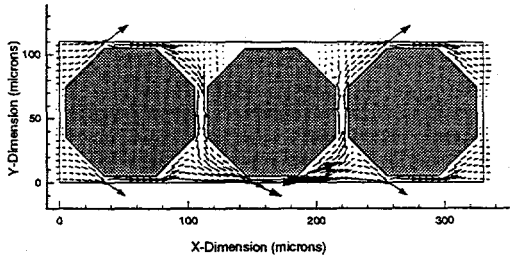

(a) Air Total Mass Flow Vectors

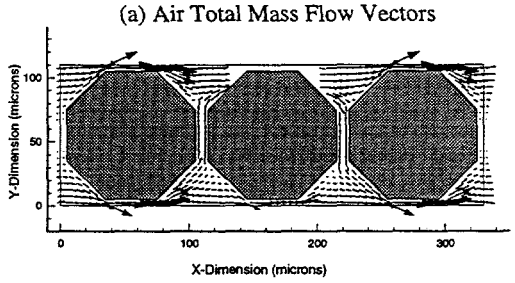

(b) Air Diffusion Mass Flow Vectors

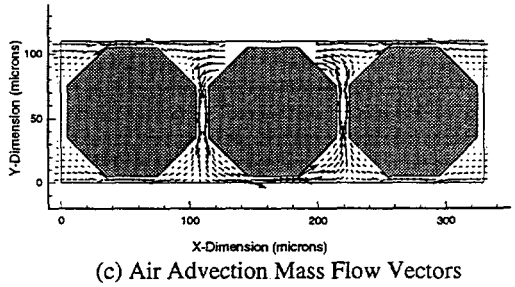

(c) Air Advection Mass Flow Vectors

Figure 13b
Air Mass Flow Vectors
for the Two-Dimensional Pore Network Model
For a Liquid Island Length of x/R=0.75

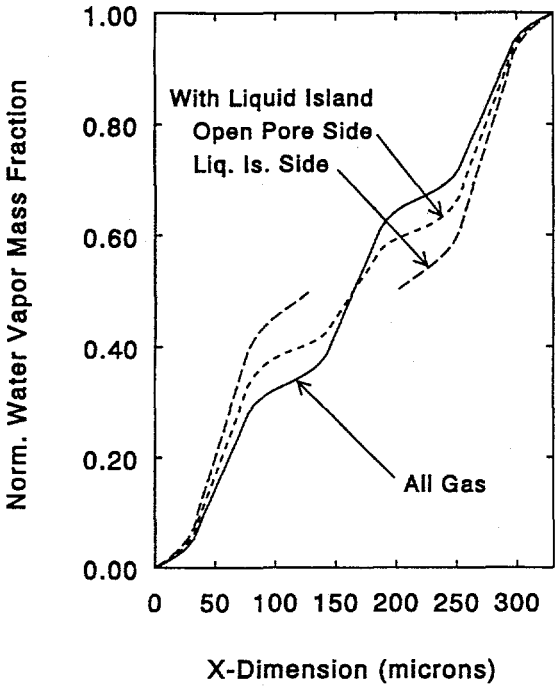

Figure 14
Normalized Water Vapor Mass Fraction Profiles

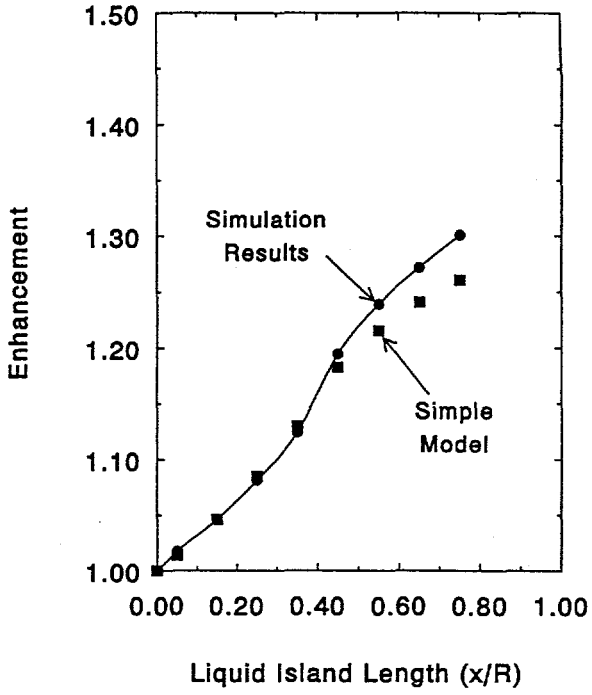

Figure 15
Enhancement of Vapor Diffusion
for the Two-Dimensional Pore Network Model

gas-liquid interface; therefore, air diffusion will be opposite and away from the interface. Because air is stagnant, a small pressure gradient will be established to balance the air diffusive flow rate. This pattern is seen in the velocity vectors. There is a significant advective air flow rate in the middle of the model, especially near the liquid island.

The water vapor concentration profiles in the x-direction in the top and bottom rows are shown in Figure 14; the water vapor mole fractions are normalized to the difference across the model. For the all-gas case, the top and bottom row conditions are identical due to symmetry. The gradient is smaller in the open portions of the pores and increases dramatically in the pore throats as expected. When the liquid island is present, the profiles are significantly different. For the bottom row with the open pore, the gradient is larger than the all-gas case in the first and last pores, indicating that the liquid island increases vapor diffusion through open pores compared to the all-gas case. In the middle pore, which is opposite the liquid island, the gradient is significantly smaller than the all-gas gradient, indicating that significant flow is diverted to the liquid island side. For the liquid island row, the gradient and the vapor diffusion rate is higher than the other cases. The profile is "missing" in the location of the liquid island because there is no vapor present. The vapor mole fraction is practically the same on either end of the liquid island, indicating that the water vapor essentially diffuses "through" the liquid island with minimal resistance. These profiles indicate that not only does vapor diffuse "through" the liquid island, but that the liquid island enhances the diffusive flow in open pores, which is also indicated in the mass flux vectors in Figure 13.

The vapor diffusion enhancement for the pore network with a single liquid island is given in Figure 15; the reason for the "kink" in the results at a liquid island length of 0.4 is due to the model pore flow area variation discussed earlier. For the present results, all flow mechanisms (diffusion plus advection plus Knudsen diffusion) are lumped together into a total "apparent" diffusive flow. The maximum enhancement is only about 30% (compared to over a factor of 10 for the single pore) because only one small liquid island is specified. The competition between a liquid island and an open pore is the primary purpose of this model.

In contrast to vapor diffusion which is enhanced by the presence of a liquid island, the diffusion of air is reduced with the introduction of a liquid island, probably due to the blocking effect of the liquid island which increases the path length for the flow of air. The porous media factor drops from 0.186 for the all-gas case to 0.136 with the shortest liquid island. The air porous media factor increases slightly as the liquid island length increases, going from 0.136 to 0.141 for the longest liquid island. The water vapor and air porous media factors as a function of liquid island length are shown in Figure 16 for the two-dimensional pore network.

IV. DISCUSSION

The results from the present pore-scale modeling investigation indicate that significant enhancement of vapor diffusion in porous media is indeed possible. The one-dimensional linear and one-dimensional pore models support the possibility of significant enhancement. Enhanced vapor diffusion in porous media may be comparable to free-space values. The two-dimensional pore network model supports the idea that vapor may preferentially flow through liquid islands rather than through open pores. Vapor is diverted from an open pore to a pore with a liquid island.

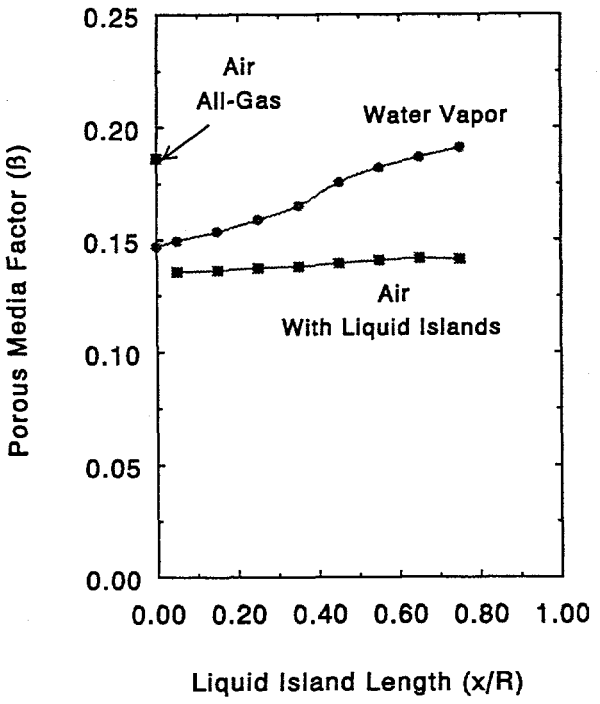

Figure 16
Water Vapor and Air Porous Media Factors (β)
for the Two-Dimensional Pore Network Model

In all three models discussed above, the liquid flow rate in the liquid island is equal to the vapor diffusion rate, resulting in steady-state flow conditions. The driving force for the liquid flow is the difference in capillary pressure between the condensing and evaporation interfaces. The location of the interfaces, and the resulting capillary pressure, is calculated by the model based on the condensation/evaporation rate and flow to and from the interface.

The present results represent the first known mechanistic calculation of enhanced vapor diffusion in porous media. Based on the present results, enhanced vapor diffusion is possible or even probable. As mentioned earlier, experimental data are being obtained to confirm the existence of enhanced vapor diffusion.

In many current engineering studies, gas and vapor diffusion are treated similarly, often using Fick's law. In addition to problems with Fick's law as discussed earlier, if enhanced vapor diffusion exists, gas and vapor diffusion should be treated differently in the presence of liquid. While gas diffusion is reduced due to the liquid, vapor diffusion may be considerably increased. At the present time, models such as developed by Jury and Letey (1979) could be used.

The enthusiasm for the present simulation results must be tempered with reality. While the present pore-scale model indicates that enhanced vapor diffusion is possible, only experimental data can confirm and quantify the process.

Additional pore-scale modeling of enhanced vapor diffusion may be useful for the evaluation of mechanisms. Three-dimensional simulations would be much more realistic than the present results. The influence of other gradients, especially temperature and pressure gradients, should be investigated. Temperature gradients are one of the assumed major drivers in enhanced vapor diffusion as discussed earlier. Other pore geometries such as staggered pores would be interesting to evaluate the effect of a different pore geometry.

V. CONCLUSIONS

Three pore-scale models of enhanced vapor diffusion in porous media (one-dimensional linear, two-dimensional single pore, and a small two-dimensional pore network) have been developed. The conclusions of the present investigation are:

1. Significant enhancement of vapor diffusion is possible in the presence of liquid islands. The enhancement increases dramatically as the length of the liquid island increases.
2. Vapor diffusion rates in pore-scale models may approach those in free space due to liquid island effects.
3. Gas and vapor diffusion should be treated differently. Gas diffusion decreases slightly in the presence of liquid islands, while vapor diffusion may be considerably enhanced.
4. Experimental data are needed to confirm and quantify enhanced vapor diffusion.
5. Additional simulations should be performed for temperature and pressure gradients, including aiding and opposing situations. Different pore geometries should be investigated. Three-dimensional modeling may be useful.

While the present model indicates that enhanced vapor diffusion is possible, only experimental data can confirm the process. As noted by Ewing and Gupta (1993), pore-scale modeling is a "useful concept rather than a physical reality". The present authors support this notion.

ACKNOWLEDGMENTS

The authors wish to thank Karsten Pruess of Lawrence Berkeley National Laboratory for providing a routine to implement the 9-point differencing scheme used in this analysis. This work was supported by the United States Department of Energy under Contract DE-AC04-94AL85000 as part of a Sandia Laboratory Directed Research and Development Project on Enhanced Vapor-Phase Diffusion in Porous Media. Sandia is a multiprogram laboratory operated by Sandia Corporation, a Lockheed Martin Company, for the United States Department of Energy.

VI. NOMENCLATURE

C	specific heat
D^K	Knudsen diffusion coefficient
D_{12}	binary diffusion coefficient
f_{vpl}	vapor pressure lowering factor
F	mass flux
g	gravity
h	enthalpy, coordinate measured from the center of the channel
J	mole flux
k	permeability, thermal conductivity
k_B	Boltzmann's constant
M	mass accumulation term, molecular weight
m_v	vapor mass flow rate
n	normal vector
ΔP	pressure difference

P pressure
q source
r pore radius
R universal gas constant, particle radius
S_g gas saturation
t time
T temperature
u internal energy
v mean molecular speed
V volume
x mole fraction

Greek
β porous media factor, phase indicator
ϱ density
κ component
σ surface tension
τ tortuosity coefficient
ϕ porosity
ω mass fraction
Γ surface
μ viscosity

Subscripts
c capillary
g gas
i gas i
l liquid
R rock
sat saturated
v vapor
w water

VII. REFERENCES

Brown, S.R., Stockman, H.W. and Reeves, S.J.,1995, "Applicability of the Reynolds equation for modeling fluid flow between rough surfaces," *Geo. Res. Let.*, 22:2537-2540.

Carman, P.C., 1952, "Diffusion and Flow of Gases and Vapours Through Micropores: IV. Flow of Capillary Condensate," *Proc. R. Soc. London,* A211, 526.

Carman, P.C., and Malherbe, P. le R., 1950, "Diffusion and Flow of Gases and Vapours Through Micropores: II. Surface Flow," *Proc. R. Soc. London*, A203, 165.

Carman, P.C., and Raal, F.A., 1951a, "Diffusion and Flow of Gases and Vapours Through Micropores: III. Surface Diffusion Coefficients and Activation Energies," *Proc. R. Soc. London*, A209, 38.

Carman, P.C., and Raal, F.A., 1951b, "Physical Adsorption of Gases on Porous Solids: I. Comparison of Loose Powder and Porous Plugs," *Proc. R. Soc. London*, A209, 59.

Cunningham, R.E., and Williams, R.J.J., 1980, Diffusion in Gases and Porous Media, Plenum Press, New York.

de Marsily, G., 1986, Quantitative Hydrogeology Groundwater Hydrology for Engineers, Academic Press, Inc., San Diego.

Dullien, F.A.L., 1992, Porous Media Fluid Transport and Pore Structure, Second Edition, Academic Press, Inc., San Diego.

Ewing, R.P., and Gupta, S.C. 1993, "Modeling percolation properties of random media using a domain network," *Water Resourc. Res.*, 29:3169-3178.

Ho, C.K., and Udell, K.S. 1992, "An experimental investigation of air venting of volatile liquid hydrocarbon mixtures from homogeneous and heterogeneous porous media," *J. Contam. Hydrol.*, Vol. 11, 291-316.

Ho, C.K., and Webb, S.W. 1997, "A Review of Porous Media Enhanced Vapor-Phase Diffusion Mechanisms, Models, and Data - Does Enhanced Vapor-Phase Diffusion Exist?" *J. Porous Media* (in press).

Jury, W.A., and Letey, Jr., J., 1979, "Water Vapor Movement in Soil: Reconciliation of Theory and Experiment," *Soil Sci. Soc. Am. J.*, Vol. 43, No. 5, pp. 823-827.

Lee, K.-H., and Hwang, S.-T., 1986, "The Transport of Condensible Vapors through a Microporous Vycor Glass Membrane," J. Colloid and Interface Science, 110:544-555.

Mason, E.A., and Malinauskas, A.P., 1983, Gas Transport in Porous Media: The Dusty-Gas Model, Chem Eng. Monograph 17, Elsevier, New York.

Philip, J.R., and deVries, D.A., 1957, "Moisture Movement in Porous Materials under Temperature Gradients," *Trans., Am. Geophys. Union*, Vol. 38, No. 2, pp. 222-232, p. 594.

Plumb, O.A., and M. Prat, 1992, "Microscopic Models for the Study of Drying of Capillary Porous Media," *Drying '92*, pp. 397-406.

Prat, M., 1993, "Percolation Model of Drying Under Isothermal Conditions in Porous Media,", *Int. J. Multiphase Flow*, 19:691-704.

Pruess, K., and G.S. Bodvarsson, 1983, "A Seven-Point Finite Difference Method for Improved Grid Orientation Performance in Pattern Steamfloods," Paper SPE-12252, Seventh Society of Petroleum Engineers Symposium on Reservoir Simulation, San Francisco, CA.

Pruess, K., and T.N. Narasimhan, 1985, "A Practical Method for Modeling Fluid and Heat Flow in Fractured Porous Media," *SPE Journal*, 25:14-26.

Pruess, K., 1991a, *TOUGH2 - A General-Purpose Numerical Simulator for Multiphase Fluid and Heat Flow*, LBL-29400, Lawrence Berkeley Laboratory.

Pruess, K., 1991b, "Grid Orientation and Capillary Pressure Effects in the Simulation of Water Injection into Depleted Vapor Zones," *Geothermics*, 20:257-277.

Pruess, K., 1995, *Proceedings of the TOUGH Workshop '95*, LBL-37200, Lawrence Berkeley Laboratory.

Rajniak, P., and Yang, R.T., 1996, "Unified Network Model for Diffusion of Condensible Vapors in Porous Media," *AIChE J.*, 42:319-331.

Ryan, D., Carbonell, R.G., and Whitaker, S., 1981, "A Theory of Diffusion and Reaction in Porous Media," *AIChE Symposium Series,* 202(77), pp. 46-62.

Sotirchos, S.V., and V.N. Burganos, 1988, "Analysis of Multicomponent Diffusion in Pore Networks," AIChE J., 34:1106-1118.

Steele, D.D., and Nieber, J.L., 1994a, "Network Modeling of Diffusion Coefficients for Porous Media: I. Theory and Model Development," *Soil Sci. Soc. Am. J.*, 58:1337-1345.

Steele, D.D., and Nieber, J.L., 1994b, "Network Modeling of Diffusion Coefficients for Porous Media: II. Simulations," *Soil Sci. Soc. Am. J.*, 58:1346-1354.

Webb, S.W., 1997, "Gas-Phase Diffusion in Porous Media - Evaluation of an Advective-Dispersive Formulation and the Dusty-Gas Model," *J. Porous Media* (in press).

Webb, S.W., and Phelan, J.M., 1997, "Effect of Soil Layering on NAPL Removal Behavior in Soil-Heated Vapor Extraction," *J. Contam. Hydrol.* (in press).

Weisz, P.B., 1975, "Diffusion Transport in Chemical Systems - Key Phenomena and Criteria," *Ber. Bunsenges, Phys. Chem.*, 79:798-806.